J. Fluid Mech. (2000), *vol.* 402, *pp.* 311–327. Printed in the United Kingdom

Suppression of vertical diffusion in strongly stratified turbulence

By YUKIO KANEDA AND TAKAKI ISHIDA†

Department of Computational Science and Engineering, Graduate School of Engineering, Nagoya University, Chikusa-ku, Nagoya 464-8603, Japan

(Received 12 January 1998 and in revised form 3 September 1999)

A spectral approximation for diffusion of passive scalar in stably and strongly stratified turbulence is presented. The approximation is based on a linearized approximation for the Eulerian two-time correlation and Corrsin's conjecture for the Lagrangian two-time correlation. For strongly stratified turbulence, the vertical component of the turbulent velocity field is well approximated by a collection of Fourier modes (waves) each of which oscillates with a frequency depending on the direction of the wavevector. The proposed approximation suggests that the phase mixing among the Fourier modes having different frequencies causes the decay of the Lagrangian two-time vertical velocity autocorrelation, and the highly oscillatory nature of these modes results in the suppression of single-particle dispersion in the vertical direction. The approximation is free from any *ad hoc* adjusting parameter and shows that the suppression depends on the spectra of the velocity and fluctuating density fields. It is in good agreement with direct numerical simulations for strongly stratified turbulence.

1. Introduction

Stratification in turbulence strongly affects transport processes in various geophysical and engineering flows. It is known that particle displacement in the vertical direction may be strongly suppressed in stably stratified turbulence, (see, e.g. Lilly, Walko & Adelfang 1974; Weinstock 1978; Kimura & Herring 1996; Vincent, Michaud & Meneguzzi 1996).

In this paper, we consider an approximation for diffusion of passive scalar in strongly stratified turbulence from the viewpoint of the spectral or two-point closure approximation. The approximation is based on the linearized approximation (or the so-called rapid distortion (RDT) approximation) and Corrsin's conjecture (1959) for passive scalar diffusion in turbulence. The linearized approximation can be solved analytically without difficulty, as done in § 2, and shows that each of the Fourier modes representing the vertical component of the velocity field generally exhibits a damped oscillation with a frequency depending on the direction of the wavevector. Cambon & Godeferd (1994) and Hanazaki & Hunt (1996) have shown that the approximation may provide good approximations for the time dependence of single-time moments. Here we apply the approximation to Eulerian two-time correlations. Corrsin's conjecture yields a simple relation between the Eulerian and Lagrangian two-time correlations. Although it has the defect of violating the invariance under random Galilean transformations as discussed in Kaneda (1993), it is also known to be in good agreement with kinematical simulations for homogeneous and isotropic

† Present address: Mitsubishi Electric Co., 6-5-66, Tebira, Wakayama 640-8686, Japan.

turbulence under certain conditions (Kraichnan 1970, 1977; Lundgren & Pointin 1976). The conjecture is applicable to the passive scalar diffusion problem not only in isotropic but also in anisotropic homogeneous stratified turbulence, as shown in § 3.

It has been argued that the suppression of vertical diffusion in strongly stratified turbulence may be due to the reduction of the magnitude of the vertical velocity component or strong horizontal turbulent mixing (see, e.g. Vincent *et al.* 1996). A simple analysis based on the present approximation suggests another mechanism which may be responsible for the suppression. According to the approximation, the Eulerian as well as the Lagrangian vertical velocity autocorrelations decay due to the mixing of the Fourier modes representing the vertical velocity component, and the suppression of vertical diffusion can occur by the highly oscillatory nature of these modes, even without reduction of the vertical velocity component, and without enhancement of horizontal turbulent mixing, as shown in § 4. The approximation explains well the strong suppression of vertical diffusion recently observed in the direct numerical simulations (DNS) by Kimura & Herring (1996). The performance of the approximation is assessed by comparisons with DNS in § 5, and it is shown to be in good agreement with DNS for strongly stratified turbulence.

2. Basic equations and linearized approximations

We consider statistically homogeneous turbulent velocity and density fields in a uniform mean density gradient that satisfy the Boussinesq approximation:

$$\frac{\partial \boldsymbol{u}}{\partial t} + (\boldsymbol{u}\cdot\nabla)\,\boldsymbol{u} = -\nabla\frac{p}{\rho_0} - \tilde{\rho}\boldsymbol{i}_3 + \nu\nabla^2\boldsymbol{u}, \tag{2.1}$$

$$\frac{\partial \tilde{\rho}}{\partial t} + (\boldsymbol{u}\cdot\nabla)\,\tilde{\rho} = \kappa\nabla^2\tilde{\rho} + N^2 u_3, \tag{2.2}$$

$$\nabla\cdot\boldsymbol{u} = 0, \tag{2.3}$$

where $\boldsymbol{u}, p, \nu$ and κ are, respectively, the velocity, pressure, kinematic viscosity and molecular diffusivity, u_i is the velocity component in the x_i-direction with (x_1, x_2, x_3) being a right-handed Cartesian coordinate system, $\boldsymbol{i}_3$ the unit vector in the x_3-direction that is anti-parallel to the vertical gravitational acceleration $\boldsymbol{g}$, ρ_0 the reference density, $\tilde{\rho}$ is proportional to the density deviation ρ' from the mean density $\overline{\rho}(x_3)$: $\tilde{\rho} = g\rho'/\rho_0$, and N the Brunt–Väisälä frequency given by $N^2 = -(g/\rho_0)(\mathrm{d}\overline{\rho}/\mathrm{d}x_3)$ with $\mathrm{d}\overline{\rho}/\mathrm{d}x_3$ being the uniform mean density gradient.

Because of the incompressibility condition (2.3), the Fourier transform $\hat{\boldsymbol{u}}(\boldsymbol{k})$ of the velocity field defined by

$$\boldsymbol{u}(\boldsymbol{x}, t) = \int \hat{u}(\boldsymbol{k}, t)\exp(\mathrm{i}\boldsymbol{k}\cdot\boldsymbol{x})\;\mathrm{d}\boldsymbol{k}, \tag{2.4}$$

may be decomposed as

$$\hat{\boldsymbol{u}}(\boldsymbol{k}, t) = \hat{\phi}_1(\boldsymbol{k}, t)\boldsymbol{e}^1 + \hat{\phi}_2(\boldsymbol{k}, t)\boldsymbol{e}^2, \tag{2.5}$$

where

$$\boldsymbol{e}^1 = \frac{\boldsymbol{i}_3\times\boldsymbol{k}}{|\boldsymbol{i}_3\times\boldsymbol{k}|}, \qquad \boldsymbol{e}^2 = \frac{\boldsymbol{k}\times\boldsymbol{e}^1}{|\boldsymbol{k}\times\boldsymbol{e}^1|}$$

(Craya 1958; Herring 1974; Métais & Herring 1989; Godeferd & Cambon 1994). For fields satisfying periodic boundary conditions, the symbol $\int \mathrm{d}\boldsymbol{k}$ is to be understood as a sum over $\boldsymbol{k}$ under appropriate normalizations. Within the linearized approximation neglecting the convective terms, (2.1) and (2.2) reduce to

$$\left(\frac{\partial}{\partial t}+\nu k^2\right)\hat{\phi}_1(\boldsymbol{k})=0, \tag{2.6}$$

$$\left(\frac{\partial}{\partial t}+\nu k^2\right)\hat{\phi}_2(\boldsymbol{k})=-\hat{\rho}(\boldsymbol{k})\sin\theta, \tag{2.7}$$

$$\left(\frac{\partial}{\partial t}+\kappa k^2\right)\hat{\rho}(\boldsymbol{k})=N^2\hat{\phi}_2(\boldsymbol{k})\sin\theta, \tag{2.8}$$

where θ is the angle between $\boldsymbol{k}$ and $\boldsymbol{i}_3$, $\hat{\rho}$ is the Fourier transform of $\tilde{\rho}$ defined similarly to (2.4), and we have used $\hat{u}_3(\boldsymbol{k})=\hat{\phi}_2(\boldsymbol{k})\sin\theta$, which is verified from (2.5).

These linearized equations can be readily solved to yield

$$\hat{\phi}_1(\boldsymbol{k},t)=\hat{\phi}_{10}(\boldsymbol{k})\,\mathrm{e}^{-\nu k^2 t}, \tag{2.9}$$

$$\hat{\phi}_2(\boldsymbol{k},t)=A\mathrm{e}^{-(\gamma_+-\mathrm{i}\alpha)t}+B\mathrm{e}^{-(\gamma_++\mathrm{i}\alpha)t}, \tag{2.10}$$

$$\hat{\rho}(\boldsymbol{k},t)=-\frac{1}{\sin\theta}[A(\gamma_-+\mathrm{i}\alpha)\mathrm{e}^{-(\gamma_+-\mathrm{i}\alpha)t}+B(\gamma_--\mathrm{i}\alpha)\mathrm{e}^{-(\gamma_++\mathrm{i}\alpha)t}], \tag{2.11}$$

where

$$\left.\begin{aligned}A&=-\frac{1}{2\mathrm{i}\alpha}[\hat{\rho}_0(\boldsymbol{k})\sin\theta+\hat{\phi}_{20}(\boldsymbol{k})(\gamma_--\mathrm{i}\alpha)],\\ B&=\frac{1}{2\mathrm{i}\alpha}[\hat{\rho}_0(\boldsymbol{k})\sin\theta+\hat{\phi}_{20}(\boldsymbol{k})(\gamma_-+\mathrm{i}\alpha)],\\ \gamma_\pm&=\tfrac{1}{2}(\nu\pm\kappa)k^2,\quad \alpha^2=N^2\sin^2\theta-\gamma_-^2,\end{aligned}\right\} \tag{2.12}$$

and $\hat{\phi}_{10},\hat{\phi}_{20}$ and $\hat{\rho}_0$ are the initial values of $\hat{\phi}_1,\hat{\phi}_2$ and $\hat{\rho}$, respectively. Here the value of α, i.e. the square root of (2.12), is to be taken appropriately. For a stably stratified turbulence with real $N>0$ and $Pr\equiv\nu/\kappa=1$, the solution can be considerably simplified. In particular, if $\hat{\rho}_0=0$, we have

$$\hat{\phi}_1(\boldsymbol{k},t)=\hat{\phi}_{10}(\boldsymbol{k})\,\mathrm{e}^{-\nu k^2 t}, \tag{2.13}$$

$$\hat{\phi}_2(\boldsymbol{k},t)=\hat{\phi}_{20}(\boldsymbol{k})\,\mathrm{e}^{-\nu k^2 t}\cos(Nt\sin\theta), \tag{2.14}$$

$$\hat{\rho}(\boldsymbol{k},t)=\hat{\phi}_{20}(\boldsymbol{k})\,\mathrm{e}^{-\nu k^2 t}N\sin(Nt\sin\theta). \tag{2.15}$$

The solutions (2.9)–(2.15) are equivalent to those by Hanazaki & Hunt (1996) which are expressed in terms of the primitive variables $(\hat{u}_1,\hat{u}_2,\hat{u}_3)$ and $\hat{\rho}$. They showed that the linearized solutions may provide good approximations for single-time covariances, especially for large N. Previously, the linearized approximation was used by Sanderson *et al.* (1991) in the analysis of the eigenvalues corresponding the two-point single-time correlation equations; however these authors recently confirmed with us that part of the analysis is incorrect (J. C. Hill, private communication). The linearized equations but with $\nu=\kappa=0$ were also analysed by Godeferd & Cambon (1994).

The solutions (2.9)–(2.15) may be used to obtain approximations not only for single-time correlations, but also for multi-time correlations, in particular for the Eulerian two-time correlation for any given initial conditions of $\boldsymbol{u}$ and $\tilde{\rho}$. Let $\hat{R}_{ij}$ be the Fourier transform defined as

$$\langle u_i(\boldsymbol{x}+\boldsymbol{r},t)u_j(\boldsymbol{x},t')\rangle = \int \hat{R}_{ij}(\boldsymbol{k};t,t')\exp(\mathrm{i}\boldsymbol{k}\cdot\boldsymbol{r})\,\mathrm{d}\boldsymbol{k}.$$

If the initial density field is uncorrelated with the velocity field so that $\langle \boldsymbol{u}(\boldsymbol{x},0)\tilde{\rho}(\boldsymbol{x}',0)\rangle = 0$ for any $\boldsymbol{x}$ and $\boldsymbol{x}'$, then the linearized approximation (2.10) with $\hat{u}_3(\boldsymbol{k}) = \hat{\phi}_2(\boldsymbol{k})\sin\theta$ yields

$$\hat{R}_{33}(\boldsymbol{k},t,t') = \mathrm{e}^{-\gamma_+(t+t')}\Bigg\{\hat{R}_{33}(\boldsymbol{k},0)\left[\frac{\gamma_-^2}{\alpha^2}\sin\alpha t\sin\alpha t' - \frac{\gamma_-}{\alpha}\sin\alpha(t+t') + \cos\alpha t\cos\alpha t'\right] + \frac{\hat{R}_{\rho\rho}(\boldsymbol{k},0)}{\alpha^2}\sin^4\theta\sin\alpha t\sin\alpha t'\Bigg\}, \qquad (2.16)$$

where $\hat{R}_{\rho\rho}(\boldsymbol{k},0) \equiv \hat{R}_{\rho\rho}(\boldsymbol{k};0,0)$ and $\hat{R}_{\rho\rho}(\boldsymbol{k};t,t')$ is the Fourier transform of $\langle\tilde{\rho}(\boldsymbol{x}+\boldsymbol{r},t)\tilde{\rho}(\boldsymbol{x},t')\rangle$ with respect to $\boldsymbol{r}$. For $Pr = 1$ and $t' = 0$, this gives

$$\hat{R}_{33}(\boldsymbol{k};t,0) = \mathrm{e}^{-\nu k^2 t}\hat{R}_{33}(\boldsymbol{k},0)\cos(Nt\sin\theta). \qquad (2.17)$$

It may be worthwhile to note here some limitations of the linearized aproximation (RDT). First, since the nonlinear terms are neglected, the excitation of modes due to nonlinear coupling is not represented in the RDT. This implies that the assumed initial characteristic length scale remains unchanged, and developing of a wider range of scales is not represented in the RDT. Second, the directional redistribution of energy due to the nonlinearity is also neglected, as is the nonlinear redistribution of energy between the velocity and density fields, and the RDT is therefore limited in its ability to describe accurately anisotropy of the flow. Such directional redistribution of energy was suggested to be responsible for the reduction of vertical velocity component in Godeferd & Cambon (1994). Although it is expected that when the Froude number $Fr \equiv u_0k_0/N$ (u_0 and k_0 are respectively the characteristic velocity and wavenumber of energy-containing eddies) is small enough or N is large enough, the effect of the nonlinearity is generally small for small t, it is difficult to get an *a priori* estimate of the effect for large t. We will therefore assess the performance of the RDT by comparison with DNS in § 5.

Since the nonlinear terms are neglected in the RDT, and the effects of viscous and diffusive terms are generally smaller than those of the nonlinearity except for very large or small wavenumber k, it is difficult to analytically justify the inclusion of the dissipative terms in the analysis. However, the analysis including them is not difficult, and it gives the asymptotic solution for the weak nonlinear limit including all the terms which may be dominant in the limit. The solution may be of theoretical interest as representing a reference state, and it may be also hoped that including them may yield a better approximation than discarding. We therefore keep the non-zero viscous and diffusive terms here.

3. Approximations for turbulent diffusivity and Lagrangian velocity correlation

As is well known, the problem of turbulent diffusivity is closely related to the Lagrangian velocity correlation. The displacement $\Delta\boldsymbol{x}$ in the time interval from t' to t of a particle may be expressed as

$$\Delta\boldsymbol{x}(t',t) \equiv \boldsymbol{x}(t') - \boldsymbol{x}(t) = \int_{t'}^{t}\boldsymbol{v}(s)\mathrm{d}s,$$

so that

$$\Delta_{ij}(t',t) \equiv \langle \Delta x_i(t',t)\Delta x_j(t',t)\rangle = \int_{t'}^{t} \mathrm{d}s \int_{t'}^{t} \mathrm{d}s' \langle v_i(s)v_j(s')\rangle, \tag{3.1}$$

where $\boldsymbol{x}(s)$ and $\boldsymbol{v}(s)$ are, respectively, the Lagrangian position and velocity at time s of the particle. Thus the covariance of the displacement can be known if the Lagrangian velocity correlation is known.

There have been extensive theoretical and experimental studies on the Lagrangian velocity correlations. Among them are studies on Lagrangian two-point two-time closure approximations (e.g. Kraichnan 1965; Kaneda 1981), which enable us to derive an approximate set of closure equations for Lagrangian two-time correlations from given dynamics governing the fluid motion such as (2.1)–(2.3). However, it requires a considerable amount of numerical computation to solve the set of equations for anisotropic turbulence. In this paper, we try a simpler kinematical approximation which is based on the conjecture by Corrsin (1959).

The approximation is obtained by noting the following relation between the Lagrangian velocity $\boldsymbol{v}$ and the Eulerian velocity $\boldsymbol{u}$:

$$\boldsymbol{v}(s) = \boldsymbol{u}(\boldsymbol{x}(s), s) = \int \mathrm{d}\boldsymbol{r}\boldsymbol{u}(\boldsymbol{r}, s)\delta(\boldsymbol{r} - \boldsymbol{x}(s)),$$

which implies

$$\langle v_i(s)v_j(s')\rangle = \int \mathrm{d}\boldsymbol{r}\langle u_i(\boldsymbol{x}(s), s)u_j(\boldsymbol{r}, s')\delta(\boldsymbol{r} - \boldsymbol{x}(s'))\rangle. \tag{3.2}$$

In the approximation of Corrsin, it is assumed that for large $|s - s'|$ the statistical dependence of the distribution of the position $\boldsymbol{x}(s')$ in (3.2) on those of $\boldsymbol{u}(\boldsymbol{x}(s), s)$ and $\boldsymbol{u}(\boldsymbol{r}, s')$ is weak, and (3.2) may therefore be approximated as

$$\langle v_i(s)v_j(s')\rangle = \int \mathrm{d}\boldsymbol{r}\langle u_i(\boldsymbol{x}(s), s)u_j(\boldsymbol{r}, s')\rangle\langle\delta(\boldsymbol{r} - \boldsymbol{x}(s'))\rangle.$$

In the wavevector space, this is equivalent for homogeneous turbulence to

$$\langle v_i(s)v_j(s')\rangle = \int \mathrm{d}\boldsymbol{k}\hat{R}_{ij}(\boldsymbol{k}, s, s')\langle \exp\left[-\mathrm{i}\boldsymbol{k} \cdot [\boldsymbol{x}(s') - \boldsymbol{x}(s)]\right]\rangle. \tag{3.3}$$

This approximation has been shown to be in good agreement with kinematic simulations for cases without helicity, not only for large $|s - s'|$, (Kraichnan 1970, 1977; Lundgren & Pointin 1976).

Equation (3.3) may be further simplified by assuming that in the evaluation of

$$\left\langle \exp\left[-\mathrm{i}\boldsymbol{k} \cdot [\boldsymbol{x}(s') - \boldsymbol{x}(s)]\right]\right\rangle = \left\langle \exp[-\mathrm{i}\boldsymbol{k} \cdot \int_{s}^{s'} \boldsymbol{v}(t)\mathrm{d}t] \right\rangle,$$

the random process $\boldsymbol{v}(t)$ may be approximated as joint normal. We then have

$$\langle v_i(s)v_j(s')\rangle = \int \mathrm{d}\boldsymbol{k}\hat{R}_{ij}(\boldsymbol{k}, s, s')\exp[-\tfrac{1}{2}k_m\Delta_{mn}(s', s)k_n] \tag{3.4}$$

(Saffman 1962; Taylor & McNamara 1971; Lundgren & Pointin 1976). By assuming (3.4) without restricting for large $|s - s'|$ and using (3.1), we can obtain closed approximations for the Lagrangian correlation $\langle v_i(s)v_j(s')\rangle$ and the displacement tensor Δ_{ij}.

In the literature, it is often assumed that the turbulence is statistically quasi-stationary in the sense that the dependence on the time t of the covariances

$\langle v_i(t+\tau)v_j(t)\rangle$ as well as $\Delta_{ij}(t+\tau,t)$ is negligible. Equations (3.1) and (3.4) then yield

$$\frac{\mathrm{d}^2\Delta_{ij}(\tau,0)}{\mathrm{d}\tau^2} = 2\int \mathrm{d}\boldsymbol{k}\hat{R}_{ij}(\boldsymbol{k},\tau;0)\exp[-\tfrac{1}{2}k_m\Delta_{mn}(\tau,0)k_n], \tag{3.5}$$

where we have assumed $\langle v_i(\tau)v_j(0)\rangle = \langle v_i(0)v_j(\tau)\rangle$.

4. Suppression of diffusivity and phase mixing

4.1. *Eulerian two-time correlation and phase mixing*

In order to get some idea of the two-time correlation functions discussed in the previous sections, it is illustrative to consider first the one-point Eulerian correlation function

$$R_{33}(t,0) \equiv \langle u_3(\boldsymbol{x},t)u_3(\boldsymbol{x},0)\rangle = \int \mathrm{d}\boldsymbol{k}\hat{R}_{33}(\boldsymbol{k},t,0), \tag{4.1}$$

for $Pr = 1$. Substituting (2.17) into (4.1) gives

$$R_{33}(t,0) = \int \mathrm{d}\boldsymbol{k}\mathrm{e}^{-\nu k^2 t}\hat{R}_{33}(\boldsymbol{k},0)\cos(Nt\sin\theta), \tag{4.2}$$

where the integration over the wavevector space may be simplified if the turbulence is not only homogeneous but also symmetric about the x_3-axis and reflection invariant, for which we may write without loss of generality

$$\hat{R}_{ij}(\boldsymbol{k},0) = P_{ij}(\boldsymbol{k})F + P_{i3}(\boldsymbol{k})P_{j3}(\boldsymbol{k})G, \tag{4.3}$$

where F and G are appropriate scalar functions depending only on k and θ, and P_{ij} is the projection operator defined by $P_{ij}(\boldsymbol{k}) = \delta_{ij} - k_ik_j/k^2$.

For example, consider the following two kinds of initial velocity spectrum tensors: one is the well known isotropic spectrum tensor given by

$$F = \tfrac{1}{3}M(k), \quad G = 0, \tag{4.4}$$

and the other is the axisymmetric spectrum tensor given by

$$F(k) = \tfrac{1}{2}M(k), \quad G(k) = -\tfrac{1}{2}M(k), \tag{4.5}$$

where M is a scalar function depending only on k. The latter spectrum may be realized by a field generated by random impulsive forces perpendicular to the symmetry axis (x_3-axis) with the correlation spectral tensor proportional to $(\delta_{ij} - \delta_{i3}\delta_{j3})M(k)$, (Saffman 1967; Chasnov 1995). Both (4.4) and (4.5) give the initial energy spectrum

$$E(k,0) = \frac{4\pi k^2}{3}M(k), \tag{4.6}$$

where

$$E(k,t) \equiv \frac{1}{2}\int \mathrm{d}\Omega\hat{R}_{ii}(\boldsymbol{k},t),$$

and $\int \mathrm{d}\Omega$ is the integral over the spherical surface of given wavenumber. Then (4.2) reduces to

$$R_{33}(t,0) = \frac{1}{2}\int_0^\infty \mathrm{d}k\mathrm{e}^{-\nu k^2 t}E(k,0)\int_0^\pi \mathrm{d}\theta\sin^3\theta\cos(Nt\sin\theta), \tag{4.7}$$

and

$$R_{33}(t,0) = \frac{3}{4}\int_0^\infty \mathrm{d}k\mathrm{e}^{-\nu k^2 t}E(k,0)\int_0^\pi \mathrm{d}\theta(\sin^3\theta - \sin^5\theta)\cos(Nt\sin\theta), \qquad (4.8)$$

for (4.4) and (4.5), respectively.

The integrals over k are of the same form in (4.7) and (4.8). The form is familiar in the study of the final period of decaying isotropic turbulence, and it is shown under fairy weak conditions that if

$$E(k,0) \sim k^n,$$

near $k = 0$, then the integral decays for large t as

$$\int_0^\infty \mathrm{d}k\mathrm{e}^{-\nu k^2 t}E(k,0) \sim t^{-(n+1)/2},$$

where the symbol '$\sim$' denotes the equality when ignoring factors independent of t.

In contrast to the integrals over k, the integrals over θ are different in (4.7) and (4.8), reflecting the difference of the initial energy spectrum. Not only for the spectra (4.4) and (4.5) but also for a wider class of axisymmetric spectra, the integral over θ in (4.2) may be generally put into the form

$$I(t) = \int_0^1 f(x)\cos(Nxt)\,\mathrm{d}x, \qquad (4.9)$$

where $x = \sin\theta$, and

$$I(t) \to 0 \qquad (4.10)$$

∞ $t \to \infty$. The form of f is determined by the velocity spectrum. For example, $f(x) \propto x^3/(1-x^2)^{1/2}$ and $f(x) \propto (x^3 - x^5)/(1-x^2)^{1/2}$, for the spectra (4.4) and (4.5), respectively.

It is to be noted that the correlation $R_{33}(t,0)$ decays even if $\nu = 0$. In the inviscid case with $\nu = \kappa = 0$, each Fourier mode does not decay but only oscillates with its own frequency determined by the direction θ of the wavevector. However, the phases of the modes may differ from each other unless $t = 0$, and the mixing of modes having different phases may result in the damping of the correlation as implied in (4.9), where the term cos(Nxt) does not decay but only oscillates with frequency determined by $Nx = N\sin\theta$, but the integral $I(t)$ over x damps as shown in (4.10).

This damping is in a sense similar to the one observed in the average

$$\langle\cos(bt)\rangle \equiv \int \cos(bt)P(b)\mathrm{d}b \qquad (4.11)$$

of random oscillators, where b is a time-independent random real number with zero mean and $P(b)$ is the probability distribution of b. For given b, cos(bt) does not decay but only oscillates. However, the average tends to zero as $t \to \infty$ under fairly weak conditions of $P(b)$ as shown by the Riemann–Lebesuge theorem. This kind of damping is well known in statistical physics, and Orszag (1977) called it stochastic relaxation in the context of studying turbulence.

In (4.11), the weighting function P represents the probability distribution of the random frequency b, while in (4.9), $x = \sin\theta$ is not random and the weighting function f represents the energy density over x. In order to distinguish this difference between the meanings of the weighting functions f and P, we will refer to the damping of (4.9) (or (4.7) and (4.8)) as that due to 'phase mixing'.

The damping due to the phase mixing occurs not only for $R_{33}(t,t')$ with $t' = 0$ as discussed above but also for general t'. When $Pr \neq 1$, we must take into account in using (2.16) that (i) $\alpha^2 = N^2 \sin^2\theta - \gamma_-^2$ (see (2.12)) can be negative so that α can be complex, and (ii) $\gamma_- \neq 0$. However, if $\gamma_-^2/N^2 = [(\nu-\kappa)k^2]^2/(4N^2) \ll 1$, then the range of θ in which $N^2\sin^2\theta - \gamma_-^2$ is negative is very small and also we may approximate α as $\alpha \approx N\sin\theta$ and γ_-/α is very small except a certain small range of θ. It is therefore expected that if

$$\frac{(\nu-\kappa)^2 k_p^4}{4N^2} \ll 1,$$

where k_p is the characteristic wavenumber of the energy-containing range, then we may in general ignore (i) and (ii) in (2.16), and (4.2) may be still available for getting a rough estimate of the correlation $R_{33}(t,0)$ for $Pr \neq 1$.

4.2. *Suppression of vertical diffusion*

The expression (3.4) is a little more complicated than (4.2). However if we introduce a bold assumption that the exponential factor in (3.4) may be discarded or approximated as

$$\exp[-\tfrac{1}{2}k_m\Delta_{mn}(s',s)k_n] \approx 1, \tag{4.12}$$

then we have

$$\langle v_i(s)v_j(s')\rangle \approx \int \mathrm{d}\boldsymbol{k}\hat{R}_{ij}(\boldsymbol{k},s,s') = R_{ij}(s,s'). \tag{4.13}$$

This implies that the Lagrangian two-time velocity autocorrelation behaves similarly to the Eulerian two-time correlation within this approximation. It is therefore expected that the damping due to the phase mixing discussed above may also occur in the Lagrangian correlation.

The approximation (4.12) cannot be valid for large k unless the displacement tensor $\Delta_{mn}(s',s)$ is very small. It may however be tolerable or work well if the integral over $\boldsymbol{k}$ in (3.4) is dominated by the wavevector range with sufficiently small k.

An approximation for the displacement tensor $\Delta_{ij}(t,0)$ may be obtained by substituting (3.4) into (3.1). In order to get a rough estimate of $\Delta_{33}(t,0)$ for large t, let us consider the case of $Pr = 1$, and neglect the viscosity and use the bold assumption (4.13). Then substituting (4.13) with (2.16) and $\alpha = N\sin\theta$ into (3.1) yields

$$\begin{aligned}
\Delta_{33}(t,0) &= \int \mathrm{d}\boldsymbol{k}\int_0^t \mathrm{d}s\int_0^t \mathrm{d}s'\left[\hat{R}_{33}(\boldsymbol{k},0)\cos\alpha s\cos\alpha s' + \frac{\hat{R}_{\rho\rho}(\boldsymbol{k},0)}{\alpha^2}\sin^4\theta\sin\alpha s\sin\alpha s'\right]\\
&= \frac{1}{2N^2}\int \mathrm{d}\boldsymbol{k}\left[\frac{\hat{R}_{33}\,(\boldsymbol{k},0)}{\sin^2\theta} + \frac{3\hat{R}_{\rho\rho}(\boldsymbol{k},0)}{N^2}\right]\\
&\quad + \frac{1}{2N^2}\int \mathrm{d}\boldsymbol{k}\left\{-\frac{\hat{R}_{33}\,(\boldsymbol{k},0)}{\sin^2\theta}\cos(2Nt\sin\theta)\right.\\
&\quad \left. + \frac{\hat{R}_{\rho\rho}(\boldsymbol{k},0)}{N^2}\,[-4\cos(Nt\sin\theta) + \cos(2Nt\sin\theta)]\right\} \qquad (4.14)\\
&= [\text{const}] + [\text{damped oscillation}],
\end{aligned}$$

where the term [const] represents the first integral of (4.14) independent of time, while the term [damped oscillation] represents the second integral which in general exhibits a sum of damped oscillations that decay due to the phase mixing. The constant depends not only on the total initial energy, but also on the form of the velocity spectrum. For example,

$$[\text{const}] = \begin{bmatrix} \dfrac{1}{2N^2}(E_0 + 3D_0) & \text{for the spectrum (4.4)} \\ \dfrac{1}{2N^2}(\tfrac{1}{2}E_0 + 3D_0) & \text{for the spectrum (4.5)} \end{bmatrix} \tag{4.15}$$

where E_0 and D_0 are respectively the initial values of the kinetic energy and the potential energy defined by

$$E_0 = \int_0^\infty E(k,0)\mathrm{d}k, \quad D_0 = \int \mathrm{d}\boldsymbol{k}\frac{R_{\rho\rho}(\boldsymbol{k},0)}{N^2}.$$

The estimate (4.14) with (4.15) shows that the mean-square displacement $\Delta_{33}(t,0)$ approaches an asymptotic value proportional to $1/N^2$ as $t \to \infty$. Such a proportionality is in agreement with previous theoretical estimates (Csanady 1964; Pearson, Puttock & Hunt 1983) which argue for $\Delta_{33}(t,0) \sim c/N^2$ for large t on the basis of Langevin models, where c is a time-independent constant. These Langevin models also include a kind of mixing of oscillations of different frequencies. For example, according to Pearson *et al.* (1983) their model gives

$$\Delta_{33}(t,0) = \int_{-\infty}^{\infty} A(\omega)(1 - \cos\, \omega t N)\Phi(\omega)\mathrm{d}\omega, \tag{4.16}$$

where $A(\omega)$ is a function of frequency ω determined by assumed constants in their model, and $\Phi(\omega)$ is determined by the pressure frequency spectrum, under appropriate normalization (see their (2.20) for the detail). Thus (4.16) also gives an expression for Δ_{33} as a sum (an integral) of oscillations with different frequencies. However, a difference between (4.14) and (4.16) is to be noted: the integration in (4.16) is over the frequency ω, and depends on the assumed frequency distribution of the pressure, whereas the integration in (4.14) is over the wavevector $\boldsymbol{k}$, representing the mixing of modes oscillating with their own frequencies depending on their wavevector directions, and shows the dependence on the wavevector spectra of the fluctuating velocity and density fields.

The decrease of $\Delta_{33}(t,0)$ with $1/N^2$ is also in agreement with the estimates (Cox, Nagata & Osborn 1969; Lilly *et al.* 1974; Weinstock 1978) which argue for $\Delta_{33}(t,0) \sim c't/N^2$, where c' is a time-independent constant. However, the time dependence of (4.14) with (4.15) is different from these estimates. The DNS by Kimura & Herring (1996) shows that $\Delta_{33}(t,0)$ is bounded and levels off at $\sim 1/N^2$. Recently, Nicolleau & Vassilicos (1999) have shown that within the linearized approximation with $\nu = \kappa = 0$, the vertical displacement is bounded in time. Their kinematical simulation also shows that $\Delta_{33}(t,0)$ approaches a constant proportional to $1/N^2$ for large t.

5. Comparison with direct numerical simulations

5.1. *Method of simulation and run conditions*

We have simulated fields obeying (2.1)–(2.3) by using the spectral method with the $\frac{2}{3}$-rule for de-aliasing in a periodic box of length 2π in the three Cartesian directions as described by Patterson & Orszag (1971). In the simulations presented below, the particles are initially at regularly located three-dimensional grid points, and then traced by solving $\mathrm{d}\boldsymbol{x}_i(t)/\mathrm{d}t = \boldsymbol{v}(\boldsymbol{x}_j,t)$, where the velocity $\boldsymbol{v}(\boldsymbol{x}_j,t)$ of each particle is computed by an interpolation method based on a spectral method. The time-marching of the fields as well as the particle motion is accomplished by a fourth-order Runge–Kutta method with a constant time increment Δt.

The initial Fourier velocity components can be generated by (2.5). We consider here two types of initial fields, say Type I (isotropic) and Type A (axisymmetric), in which the initial amplitudes $\hat{\phi}_1$ and $\hat{\phi}_2$ in (2.5) are given by

$$\hat{\phi}_1(\boldsymbol{k}) = \left[\frac{M(k)}{3}\right]^{1/2} \exp(2\mathrm{i}\pi\chi_1), \quad \hat{\phi}_2(\boldsymbol{k}) = \left[\frac{M(k)}{3}\right]^{1/2} \exp(2\mathrm{i}\pi\chi_2), \quad \text{for Type I},$$

and

$$\hat{\phi}_1(\boldsymbol{k}) = \left[\frac{M(k)}{2}\right]^{1/2} \exp(2\mathrm{i}\pi\chi_1), \quad \hat{\phi}_2(\boldsymbol{k}) = \frac{k_3}{k}\left[\frac{M(k)}{2}\right]^{1/2} \exp(2\mathrm{i}\pi\chi_2), \quad \text{for Type A},$$

under the constraint of the reality condition $\boldsymbol{u}^*(\boldsymbol{k},0) = \boldsymbol{u}(-\boldsymbol{k},0)$, where

$$M(k) = \frac{4}{\pi}\left(\frac{2}{\pi}\right)^{1/2} u_0^2 k_p^{-5} k^2 \exp\left[-2\left(\frac{k}{k_p}\right)^2\right], \tag{5.1}$$

$u_0 = 1.242, k_p = 4.767$, the symbol * denotes the complex conjugate, and χ_1 and χ_2 are uniformly distributed random numbers between 0 and 1, and statistically independent of each other (Chasnov 1995). The initial energy spectrum $\hat{R}_{ij}(\boldsymbol{k},0)$ is then given by (4.3) with (4.4) for Type I and with (4.5) for Type A, as may be verified by taking the contractions $e_i^1 e_j^1 \hat{R}_{ij}$ and $e_i^2 e_j^2 \hat{R}_{ij}$, and using $P_{ij}(\boldsymbol{k}) = e_i^1 e_j^1 + e_i^2 e_j^2$. For both Types I and A, $\langle \boldsymbol{u} \cdot \boldsymbol{u} \rangle = 2\int E(k,0)\mathrm{d}k = u_0^2$.

The initial density fluctuation is set to zero except for the case shown in figure 4, and we use the following parameter values: the Brunt–Väisälä frequency N is given by $N^2 = 10, 100$ or 1000, and $\nu = 0.005, \kappa = 0.005$. These parameter values give the Prandtl number $Pr \equiv \nu/\kappa = 1$, the initial Reynolds number $Re \equiv u_0/(\nu k_p) \simeq 52$, and the initial Froude number $Fr \equiv u_0 k_p/N \simeq 1.87$, 0.59 or 0.19. The number of tracer particles m and time increment Δt in the time marching are set to be $m = 512$ and $\Delta t = 0.005$. In order to check the effect of m and Δt, we have also performed simulations with doubling m or reducing Δt by half for the case $N^2 = 1000$ with initial field of Type I. No significant change was observed for the changes.

The above values for k_p, N^2, ν and κ were also used in Kimura & Herring (1996, hereafter referred as KH) in their DNS. There are however some differences between our runs and KH's. First, the initial Reynolds number, and the numbers of mesh points (64^3) and tracer particles ($m = 512$) are smaller, and the time of particle tracing is somewhat shorter in the former. Second, the introduction of the stratification and density fluctuations as well as the particle release are done at $t = 0$ in our runs, whereas they are done after the enstrophy reaches its peak value in KH.

In the present study, we wish to know the possible effect of the spectrum $R_{ij}(\boldsymbol{k})$ on the turbulent diffusivity. However, neither the velocity nor the density fluctuation spectrum at the time when the fluctuations and stratification are introduced or the particles are released is available from KH. We therefore decided to perform simulations presented below, in which the information on the spectra is available, and we can consider not only isotropic but also anisotropic initial conditions (KH treated only isotropic initial condition). In spite of the differences noted above, the present and KH's DNS show at least qualitatively similar statistics regarding the vertical turbulent diffusivity and Lagrangian velocity (cf. figures 4 and 7 in KH and figures 2 and 3 shown below); they exhibit strong suppression of vertical diffusion for large

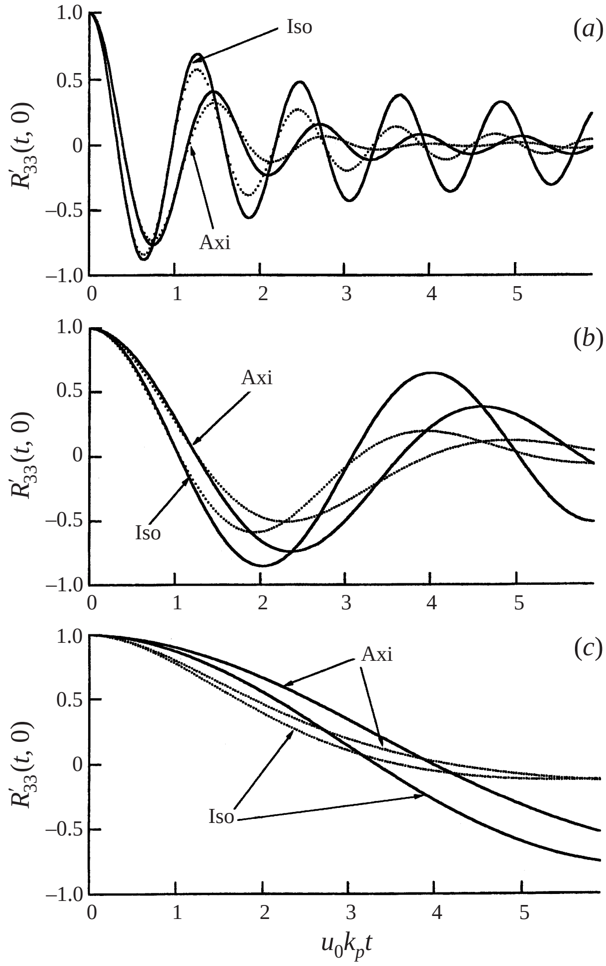

FIGURE 1. Normalized Eulerian correlation $R'_{33}(t, 0)$ vs. time t for (*a*) $N^2 = 1000$, (*b*) $N^2 = 100$ and (*c*) $N^2 = 10$; solid and dotted lines are respectively theoretical and DNS values. Values for the runs with the initial field of Type I and Type A are labelled as Iso and Axi, respectively.

N^2. The similarity suggests that the differences are unlikely to be significant for the following discussion especially for large N^2, and gives a justification for our using the simulation results here.

5.2. *Simulation results*

Figures 1(*a*), 1(*b*) and 1(*c*) show the normalized Eulerian two-time correlation

$$R'_{33}(t, 0) \equiv \frac{\langle u_3(\boldsymbol{x}, t) u_3(\boldsymbol{x}, 0)\rangle}{\langle u_3^2(\boldsymbol{x}, 0)\rangle},$$

for $N^2 = 1000, 100$, and 10, respectively, from DNS and the linearized approximation (4.2). The DNS values show that the correlation decays in an oscillatory manner in time t, and the period of oscillation is shorter for larger N^2. They also show that the correlation decays faster in the runs with initial condition of Type A (or simply runs of Type A) than in the runs of Type I, for large N^2. Thus the decay depends on the initial energy spectrum. These properties are well captured by the

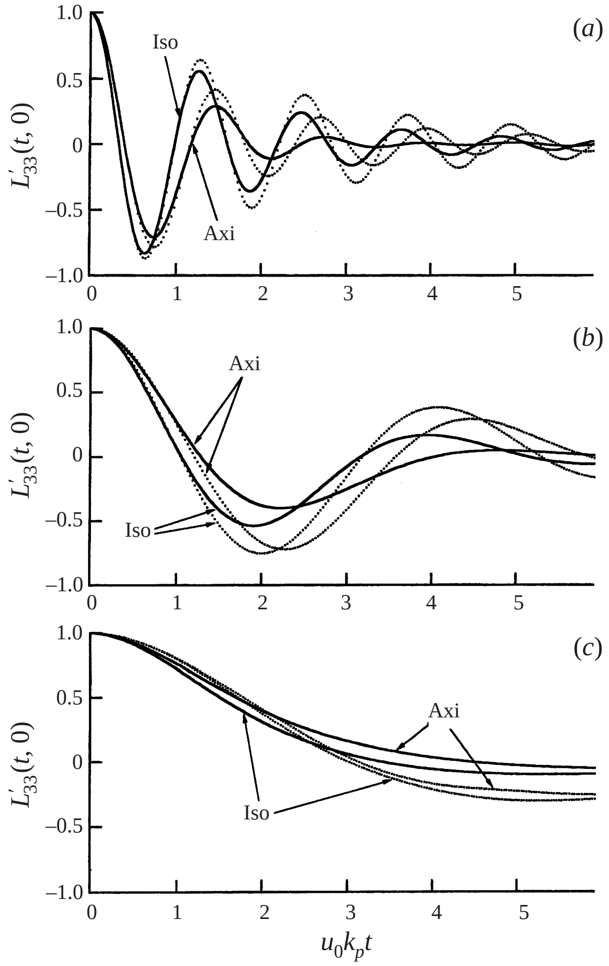

FIGURE 2. The same as figure 1, but for the normalized Lagrangian two-time correlation.

linearized approximation, which is seen to be in fairly good agreement with the DNS especially for large N^2. The same is also true for the normalized Lagrangian two-time correlation

$$L'_{33}(t,0) \equiv \frac{\langle v_3(\boldsymbol{x},t)v_3(\boldsymbol{x},0)\rangle}{\langle v_3^2(\boldsymbol{x},0)\rangle},$$

shown in figure 2. Here the theoretical values for the Lagrangian correlation are obtained by solving the closed set of equations (3.1) and (3.4) for the Eulerian spectrum given by (2.16).

In order to check the influence of the Prandtl number we have also simulated fields and correlations under the same conditions as those for the runs of Type I, but with $\kappa = 0.025(Pr = 5)$ or $\kappa = 0.001(Pr = 0.2)$. In all of the runs, the value of $[(\nu - \kappa)k_p^2]^2/(4N^2)$ is very small, and the simulated values of the Eulerian and Lagrangian correlations are not significantly different from those shown in figures 1 and 2, as would be expected from the discussion in the last paragraph of §4.1, and the figures are omitted here.

Figure 3 compares the mean-square particle displacements, $\Delta_{33}(t,0) \equiv \langle [x_3(t) -$

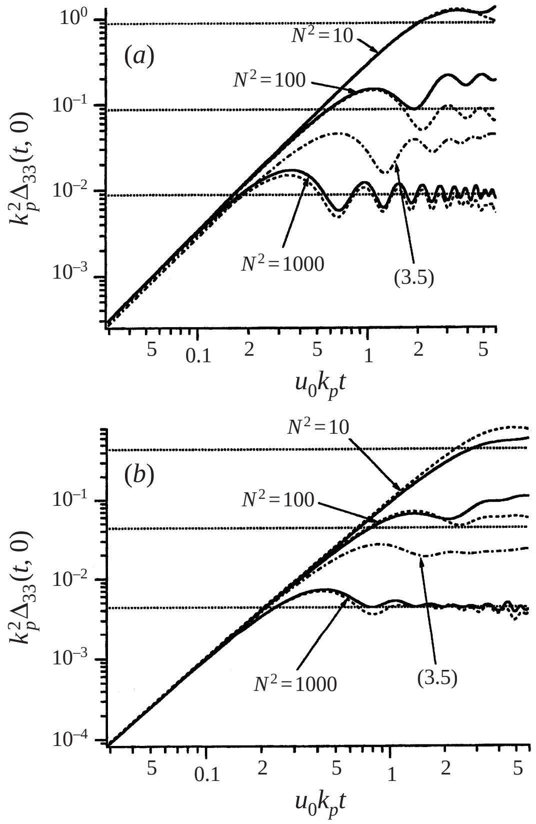

FIGURE 3. Mean-square displacement $\Delta_{33}(t,0)$ vs. time t for the values of N^2 labelled in the figure and for (a) the runs of Type I, and (b) the runs of Type A; solid and dotted lines are respectively theoretical and DNS values. The line labelled as (3.5) shows the values for $N^2 = 1000$ based on (3.5). The straight lines are asymptotic values from (4.15).

$x_3(0)]^2\rangle$ from DNS and the theoretical values obtained by (3.1) and (3.4) with (2.16) or (2.17). As seen in the figure, the theoretical values are in good agreement with the DNS, especially for large N^2. For $N^2 = 1000$, it is observed that the displacement is strongly suppressed. The asymptotic value for large t is in fairly good agreement with the bold estimate (4.15), in which the asymptotic value is proportional to $1/N^2$. From the comparison between figures 3(a) and 3(b), the asymptotic values are seen to be not the same. This as well as the estimate (4.14) suggests the value depends on the spectrum. The DNS value for $N^2 = 1000$ shows a slight decrease with time. Such a decrease is also seen in the DNS by KH.

Figures 1, 2, and 3 suggest that the agreement between the theory and DNS is better in figure 3, especially in figure 3(b), than in figures 1 and 2. This is not surprising in view of the following consideration. The highly oscillatory nature of the vertical velocity component for large N^2, or that of the two-time correlation spectrum $\hat{R}_{33}(\boldsymbol{k}, s, s')$ for large $|N \sin\theta|$ is well captured by the RDT, although the difference between the RDT and the DNS solutions for the velocity field or $\hat{R}_{33}(\boldsymbol{k}, s, s')$ as an initial value problem may increase with time. Due to this oscillatory nature, the contribution from the range of large times s and s' to the integral for Δ_{33} in (3.1) may be not so significant, and thereby $\Delta_{33}(t,0)$ at large t may be not very sensitive to the error from the theory at large s and s'.

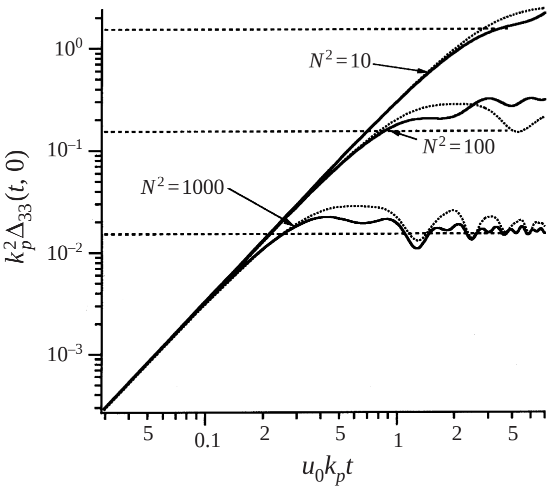

FIGURE 4. The same as figure 3(*a*), but for the case of non-zero initial density fluctuation.

In order to check the validity of the simplifying assumption of quasi-stationarity implied by (3.5), the values from the use of (3.5) instead of (3.4) are also shown for $N^2 = 1000$ in the figure. It is seen that the agreement is poor even for $N^2 = 1000$, and the assumption may not be justifiable.

Figure 4 shows the comparison for cases similar to the runs of Type I but with non-zero initial density fluctuation spectrum

$$\hat{R}_{\rho\rho}(\boldsymbol{k}, 0) = \frac{CE(k, 0)}{4\pi k^2},$$

where $E(k, 0)$ is given by (4.6) and (5.1), and the constant C is so chosen that $D_0 = E_0/4$, i.e. $C = \frac{1}{4}N^2$. The figure again shows a good agreement between the theoretical values and DNS for large N^2. The comparison between the DNS values in figures 3(*a*) and 4 shows that the asymptotic value of $\Delta_{33}(t, 0)$ for large t may depend not only on the initial kinetic energy E_0 but also on the potential energy D_0, in agreement with the estimate (4.15).

These figures suggest that the agreement with the asymptotic estimate (4.15) for large t and DNS are generally good within the observed time interval for large N^2. There remains the possibility that due to neglected nonlinearity, the asymptotic behaviour for much longer time may be different. To check such a possibility, time integration for much longer time would be necessary.

One might think that the suppression might be due to strong reduction of the magnitude of the vertical velocity component. However, as shown in figure 5 for the runs of Type I, the normalized Eulerian single-point moment

$$R'_{33}(t) \equiv \frac{\langle u_3(\boldsymbol{x}, t)u_3(\boldsymbol{x}, t)\rangle}{\langle u_3(\boldsymbol{x}, 0)u_3(\boldsymbol{x}, 0)\rangle}$$

remains at order unity in the observed time range, and the observed reduction/change of the vertical velocity magnitude is clearly insufficient to explain the strong suppression of the vertical displacement for large N^2, as seen in figure 3.

One might also think that the suppression might be due to strong anisotropy of the velocity field, or strong horizontal mixing as discussed by Vincent *et al.* (1996).

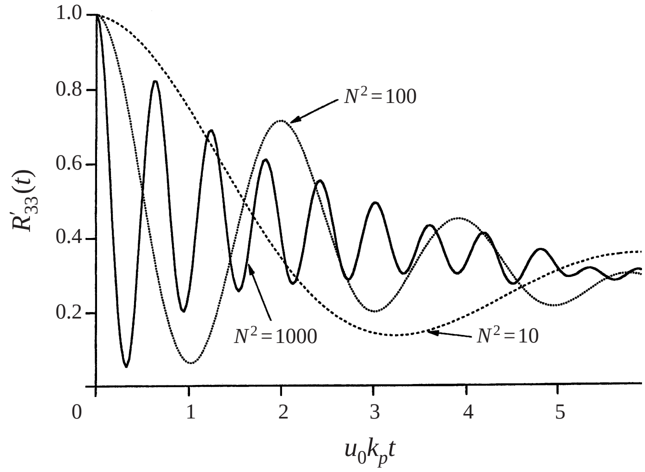

FIGURE 5. Normalized mean-square vertical velocity $R'_{33}(t)$ vs. time for $N^2 = 10, 100$ and 1000 and the runs of Type I.

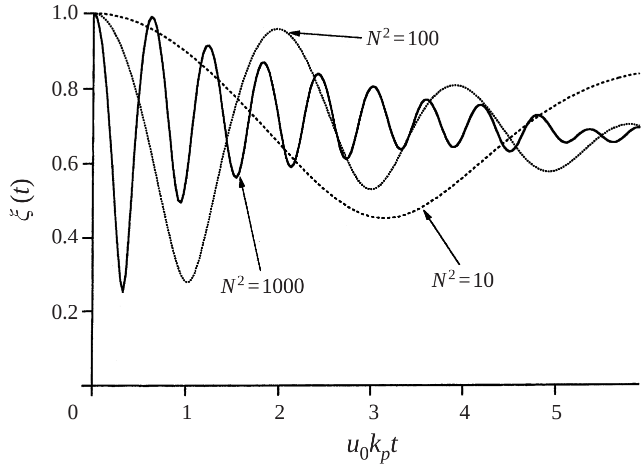

FIGURE 6. The anisotropy ratio ξ defined by (5.2) vs. time for the runs of Type I.

The anisotropy may be measured by

$$\xi(t) = \left[\frac{2\langle u_3^2\rangle}{\langle u_1^2\rangle + \langle u_2^2\rangle}\right]^{1/2}, \tag{5.2}$$

and is shown in figure 6 for the runs of Type I. It shows that the ratio ξ remains at order unity in the observed time range, and suggests that the anisotropy or horizontal mixing is not essential for the suppression observed in figure 3.

The above results do not imply that in general either the reduction of vertical velocity or a strong flow anisotropy plays any significant role. What they suggest is that, at least in the case studied here, these effects, as observed in figures 5 and 6, are insufficient to explain the strong suppression as observed in figure 3 for large N^2.

6. Results and discussion

The comparisons with DNS in the previous section show that the approximation based on (2.16) (or (2.17)) and (3.4) agrees well with the DNS, at least for large N^2.

The approximation shows that the Eulerian as well as the Lagrangian vertical velocity autocorrelations decay due to the mixing of the (damped) oscillating Fourier modes representing the vertical component of the velocity field whose frequencies depend on the wavevector directions, and the suppression of the displacement in the vertical direction depends on how the modes are mixed, i.e. it depends on the velocity spectrum. The time dependence of Lagrangian as well as the Eulerian two-time velocity correlation, and the displacement tensor Δ_{ij} differ for different velocity spectrum. It therefore seems difficult to explain the differences by using only one-point quantities such as the total energy. The approximation suggests the necessity of taking into account the spectrum or two-point information, and also suggests that once the spectrum information is taken into account, then we can obtain a reasonable approximation without introducing any *ad hoc* adjusting parameter, at least for large N^2.

It is often assumed in the literature that the mean square of particle displacement is proportional to the time difference such as

$$\Delta_{ij}(t, 0) \propto D_{ij} t,$$

for large t, where D_{ij} is a constant called the turbulent (or eddy) diffusion constant. This approximation is based on the assumption that the Lagrangian two-time correlation is stationary. However, the Eulerian correlation given by (2.16) and used in (3.4) is clearly non-stationary. It is therefore difficult to justify this assumption of stationarity for large N^2, and the non-stationarity results in poor agreement between DNS and the approximation based on (3.5), at least in the observed time range shown in figure 3.

For moderate or small N^2, it is expected that we need take into account the nonlinearity which is neglected in the linearized approximation. It would be interesting to try approximations taking into account both the nonlinearity and the spectrum information, and this is left for future studies.

The authors are grateful to Dr T. Ishihara, Mr K. Gotoh for their assistance in computational debugging and making the figures, and to Professor J. C. Hill, Dr Vassilicos and Dr K. Beronov for useful discussions. This work was supported by 'Research for the Future' Program of the Japan Society for the Promotion of Science under the project JSPS-RFTF97P01101, and also by a Grant-in-Aid for Scientific Research from the Ministry of Education, Science, Sports and Culture of Japan (No. 09440076). The computation was carried out by the VPP500 system at the computer center of Nagoya University.

REFERENCES

Cambon, C. & Godeferd, F. S. 1994 Inertial transfers in freely decaying, rotating, stably stratified, and magnetohydrodynamic turbulence. In *Progress in Turbulence Research* (ed. H. Branover & Y. Unger), vol. 162, pp. 150–168. AIAA.

Corrsin, S. 1959 Progress report on some turbulent diffusion research. In *Atmospheric Diffusion and Air Pollution* (ed. F. N. Frenkiel & P. A. Sheppard). Advances in Geophysics, vol. 6, pp. 161–164. Academic.

Cox, C. Y., Nagata, Y. & Osborn, T. 1969 Oceanic fine structure and internal waves. Papers in dedication to Prof. Michitaka Uda. *Bull. Japan Soc. Fish. Oceanogr., Tokyo* **1**, 67–71.

Chasnov, J. R. 1995 The decay of axisymmetric homogeneous turbulence. *Phys. Fluids* **7**, 600–605.

Craya, A. 1958 *Contribution à l'Analyse de la Turbulence Associée à des Vitesse Moyennes*. P.S.T. Ministère de l'Air (Fr), 345 pp.

Csanady, G. T. 1964 Turbulent diffusion in a stratified fluid. *J. Atmos. Sci.* **21**, 439–447.

Godeferd, F. S. & Cambon, C. 1994 Detailed investigation of energy transfers in homogeneous stratified turbulence. *Phys. Fluids* **6**, 2084–2100.

Hanazaki, H. & Hunt, J. C. R. 1996 Linear processes in unsteady stably stratified turbulence. *J. Fluid Mech.* **318**, 303–337.

Herring, J. R. 1974 Approach of axisymmetric turbulence to isotropy. *Phys. Fluids* **17**, 859–872.

Kaneda, Y. 1981 Renormalized expansions in the theory of turbulence with the use of the Lagrangian position function. *J. Fluid Mech.* **107**, 131–145.

Kaneda, Y. 1993 Lagrangian and Eulerian time correlations in turbulence. *Phys. Fluids* A **5**, 2835–2845.

Kimura, Y. & Herring, J. R. 1996 Diffusion in stably stratified turbulence. *J. Fluid Mech.* **328**, 253–269 (referred to herein as KH).

Kraichnan, R. H. 1965 Lagrangian-history closure approximation for turbulence. *Phys. Fluids* **8**, 575–598.

Kraichnan, R. H. 1970 Diffusion by a random velocity field. *Phys. Fluids* **13**, 22–31.

Kraichnan, R. H. 1977 Lagrangian velocity covariance in helical turbulence. *J. Fluid Mech.* **81**, 385–398.

Lilly, D. K., Walko D. E. & Adelfang, S. 1974 Stratospheric mixing estimated from high-altitude turbulence measurements. *J. Appl. Met.* **13**, 488–493.

Lundgren, T. S. & Pointin, Y. B. 1976 Turbulent self-diffusion. *Phys. Fluids* **19**, 355–358.

Métais, O. & Herring, J. R. 1989 Numerical simulations of freely evolving turbulence in stably stratified fluids. *J. Fluid Mech.* **202**, 117–148.

Nicolleau, F. & Vassilicos, J. C. 1999 Turbulent diffusion in stably stratified non-decaying turbulence. *J. Fluid Mech.* (submitted).

Orszag, S. A. 1977 Lectures on the statistical theory of turbulence. In *Fluid Dynamics* (ed. R. Balian & J.-L. Peube), pp. 235–374. Gordon and Breach.

Patterson, G. S. & Orszag, S. A. 1971 Spectral calculations of isotropic turbulence: efficient removal of aliasing interactions. *Phys. Fluids* **14**, 2538–2541.

Pearson, H. J., Puttock, J. S. & Hunt, J. C. R. 1983 A statistical model of fluid-element motions and vertical diffusion in a homogeneous stratified turbulent flow. *J. Fluid Mech.* **129**, 219–249.

Saffman, P. G. 1962 An approximate calculation of the Lagrangian auto-correlation coefficient for stationary homogeneous turbulence. *Appl. Sci. Res.* A **11**, 245–255.

Saffman, P. G. 1967 The large-scale structure of homogeneous turbulence. *J. Fluid Mech.* **27**, 581–593.

Sanderson, R. C., Leonard, A. D., Herring, J. R. & Hill J. C. 1991 Fossil and Active Turbulence. In *Turbulence and Coherent Structures* (ed. O. Métais & M. Lesieur), pp. 429–448. Kluwer.

Taylor, J. B. & McNamara, B. 1971 Plasma diffusion in two dimensions. *Phys. Fluids* **14**, 1492–1499.

Vincent, A., Michaud, G. & Meneguzzi, M. 1996 On the turbulent transport of a passive scalar by anisotropic turbulence. *Phys. Fluids* **8**, 1312–1320.

Weinstock, J. 1978 Vertical turbulent diffusion in a stably stratified fluid. *J. Atmos. Sci.* **35**, 1022–1027.